

Diels–Alder Reactions of Masked *o*-Benzoquinones: New Experimental Findings and a Theoretical Study of the Inverse Electron Demand Case[‡]

Odón Arjona,[§] Rocío Medel,[§] Joaquín Plumet,^{*,§} Rafael Herrera,[‡]
Hugo A. Jiménez-Vázquez,[†] and Joaquín Tamariz^{*,†}

Departamento de Química Orgánica, Facultad de Química, Universidad Complutense, 28040 Madrid, Spain, Instituto de Investigaciones Químico-biológicas, Universidad Michoacana de San Nicolás de Hidalgo, Edif. B-1, Ciudad Universitaria, Francisco J. Mujica S/N, 58066 Morelia, Michoacan, Mexico, and Departamento de Química Orgánica, Escuela Nacional de Ciencias Biológicas, Instituto Politécnico Nacional, Prol. Carpio y Plan de Ayala, 11340 México, D.F., Mexico

plumety@quim.ucm.es

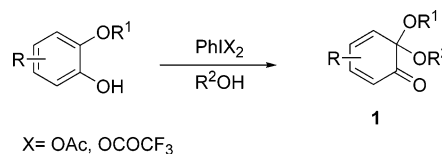
Received September 29, 2003

Diels–Alder reactions of the masked *o*-benzoquinone (MOB) **2** with vinylen carbonate (**3**), the bicyclic derivatives **4**, **5**, and **6**, and the intramolecular version of the 2-hydroxymethylfuran–MOB Diels–Alder reaction are described. In addition, a theoretical study of the Diels–Alder reactions of MOBs with enol and thioenol ethers is presented.

Masked *o*-benzoquinones (MOBs) **1** are a synthetically useful class of cyclohexa-2,4-dienones.¹ These compounds can be generated by in situ oxidation of readily available α -alkoxy phenols, using hypervalent iodine reagents in the presence of an alcohol (Scheme 1).²

MOBs have been shown to be efficient 4π components in Diels–Alder reactions undergoing regio- and stereo-selective cycloaddition processes with electron-deficient³ and electron-rich dienophiles.⁴ Other 2π components used in these reactions have been heteroaromatic compounds such as furan,⁵ indole,⁶ pyrrole,⁷ and thiophene⁸ deriva-

SCHEME 1



tives. Hetero-⁹ and intramolecular^{3g,10} Diels–Alder reactions have also been considered.

In several cases the resulting bicyclo[2.2.2]octenone derivatives have been used as starting materials for the synthesis of different targets, including polysubstituted cyclohexenes,¹¹ *cis*-decalins,¹² bicyclo[4.2.2]decanones,^{12g} the triquinane ring system,¹³ and highly functionalized tricyclic compounds.¹⁴ It should be pointed out that these Diels–Alder processes were a key step in several complex synthetic sequences, such as in the syntheses of clerodane

[‡] This paper is dedicated to Professor Jose Luis Soto.

[§] Universidad Complutense.

[‡] Universidad Michoacana de San Nicolás de Hidalgo.

[†] Instituto Politécnico Nacional.

(1) For selected recent reviews, see: (a) Liao, C. C. *Acc. Chem. Res.* **2002**, *35*, 856–866. (b) Quideau, S.; Pouységu, L. *Org. Prep. Proced. Int.* **1999**, *31*, 617–680. (c) Liao, C. C. *Modern Methodology in Organic Synthesis*; Kodansha: Tokyo, Japan, 1992; p 409.

(2) (a) Kürti, L.; Herczegh, P.; Visy, J.; Simonyi, M.; Antus, S.; Pelter, A. *J. Chem. Soc., Perkin Trans. 1* **1999**, 379–380. (b) Varvoglis, A. *Hypervalent Iodine in Organic Synthesis*; Academic Press: San Diego, CA, 1997. (c) Bodajla, M.; Jones, G. R.; Ramsden, C. A. *Tetrahedron Lett.* **1997**, *38*, 2573–2576. (d) Stang, P. J.; Zhdkankin, V. V. *Chem. Rev.* **1996**, *96*, 1123–1178.

(3) (a) Lai, C. H.; Shen, Y. L.; Wang, M. N.; Kameswara Rao, N. S.; Liao, C. C. *J. Org. Chem.* **2002**, *67*, 6493–6502. (b) Lai, C. H.; Lin, P. Y.; Peddinti, R. K.; Liao, C. C. *Synlett* **2002**, 1520–1522. (c) Chittimalla, S. K.; Liao, C. C. *Synlett* **2002**, 565–568. (d) Liao, C. C.; Chu, C. S.; Lee, T. H.; Rao, P. D.; Ko S.; Song, L. D.; Shiao, H. C. *J. Org. Chem.* **1999**, *64*, 4102–4110. (e) Yang, M. S.; Chang, S. Y.; Lu, S. S.; Rao, P. D.; Liao, C. C. *Synlett* **1999**, 225–227. (f) Lai, C. H.; Shen, Y. L.; Liao, C. C. *Synlett* **1997**, 1351–1352. (g) Chu, C. S.; Lee, T. H.; Liao, C. C. *Synlett* **1994**, 635–636.

(4) (a) Gao, S. Y.; Ko, S.; Lin, Y. L.; Peddinti, R. K.; Liao, C. C. *Tetrahedron* **2001**, *57*, 297–308. (b) Gao, S. Y.; Lin, Y. L.; Rao, P. D.; Liao, C. C. *Synlett* **2000**, 421–423. (c) Arjona, O.; Medel, R.; Plumet, J. *Tetrahedron Lett.* **1999**, *40*, 8431–8433.

(5) (a) Chou, Y. Y.; Peddinti, R. K.; Liao, C. C. *Org. Lett.* **2003**, *5*, 1637–1640. (b) Chen, C. H.; Rao, P. D.; Liao, C. C. *J. Am. Chem. Soc.* **1998**, *120*, 13254–13255.

(6) Hsieh, M. F.; Rao, P. D.; Liao, C. C. *Chem. Commun.* **1999**, 1441–1442.

(7) Hsieh, M. F.; Peddinti, R. K.; Liao, C. C. *Tetrahedron Lett.* **2001**, *42*, 5481–5484.

(8) Lai, C. H.; Ko, S.; Rao, P. D.; Liao, C. C. *Tetrahedron Lett.* **2001**, *42*, 7851–7854.

(9) Lin, K. C.; Liao, C. C. *Chem. Commun.* **2001**, 1624–1625.

(10) (a) Lin, K. C.; Shen, Y. L.; Kameswara Rao, N. S.; Liao, C. C. *J. Org. Chem.* **2002**, *67*, 8157–8165. (b) Chu, C. S.; Lee, T. H.; Rao, P. D.; Song, L. D.; Liao, C. C. *J. Org. Chem.* **1999**, *64*, 4111–4118.

(11) (a) Arjona, O.; Medel, R.; Plumet, J. *Tetrahedron Lett.* **2001**, *42*, 1287–1288. (b) Lee, T. H.; Rao, P. D.; Liao, C. C. *Chem. Commun.* **1999**, 801–802.

(12) (a) Sutherland, H. S.; Higgs, K. C.; Taylor, N. J.; Rodrigo, R. *Tetrahedron* **2001**, *57*, 309–317. (b) Carlini, R.; Higgs, K.; Rodrigo, R.; Taylor, N. *Chem. Commun.* **1998**, 65–66. (c) Hsu, P. Y.; Lee, Y. C.; Liao, C. C. *Tetrahedron Lett.* **1998**, 659–662. (d) Rao, P. D.; Chen, C. H.; Liao, C. C. *Chem. Commun.* **1998**, 155–156. (e) Hsu, P. Y.; Liao, C. C. *Chem. Commun.* **1997**, 1085–1086. (f) Carlini, R.; Higgs, K.; Older, C.; Randhawa, S. *J. Org. Chem.* **1997**, *62*, 2330–2331. (g) Lee, T. H.; Liao, C. C.; Liu, W. C. *Tetrahedron Lett.* **1996**, *37*, 5897–5900.

(13) (a) Hsu, D. S.; Rao, P. D.; Liao, C. C. *Chem. Commun.* **1998**, 1795–1796. (b) Hwang, J. T.; Liao, C. C. *Tetrahedron Lett.* **1991**, *32*, 6583–6586.

(14) (a) Chen, Y. K.; Peddinti, R. K.; Liao, C. C. *Chem. Commun.* **2001**, 1340–1341. (b) Rao, P. D.; Shen, C. H.; Liao, C. C. *Chem. Commun.* **1999**, 713–714.

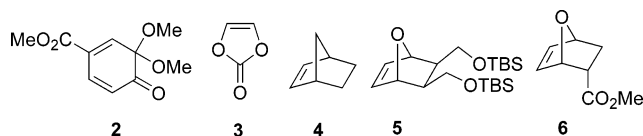


FIGURE 1. Structures of diene **2** and dienophiles **3–6**.

diterpenic acids,¹⁵ the iridoid forsythide aglycon dimethyl ester,¹⁶ pallescensin B,¹⁷ eremopetasidione,¹⁸ the *Lycopodium* alkaloid megallanine,¹⁹ reserpine (formal synthesis),²⁰ the calicheamicinone aglycon,²¹ kadsurenone, denudatin B, liliflol B, *O*-methyliliflodione,²² asatone,²³ the carbocyclic core of CP-263,114,²⁴ xestoquinone,^{12a,f} and halenoquinone.²⁵

Several theoretical approaches have been considered to explain the regio- and stereoselective aspects of the reaction, including simple FMO models^{3d,4a} and quantum mechanical calculations of transition states and possible intermediates of these reactions.²⁶ In some cases, secondary orbital interactions have been invoked to explain the total *endo* stereoselectivity observed.^{3d}

As a new contribution to this chemistry, we wish to address in this paper the Diels–Alder reactions of the masked *o*-benzoquinone **2** with vinylene carbonate (**3**), the bicyclic derivatives **4**, **5**, and **6** (Figure 1), and the hitherto not considered intramolecular version of the furan–MOB Diels–Alder reaction. On the other hand, we

previously described, for the first time, the Diels–Alder reactions of **2** with enol and thioenol ethers.^{4c} A theoretical study of this process is also presented.

Results

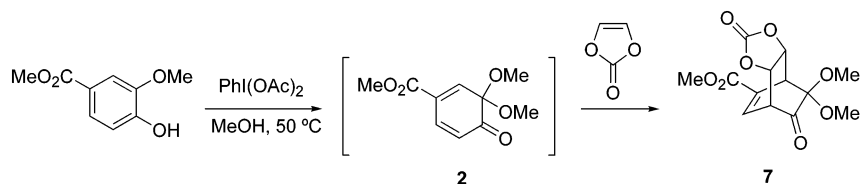
The reaction of **3** with MOB **2** afforded the expected tricyclic derivative **7** in a totally stereoselective fashion, albeit in low yield (27% isolated). Dimerization of **2** (35% of the corresponding dimer was obtained) was the main competitive process (Scheme 2).

The stereochemical assignment of **7** was confirmed by correlation of its ¹H NMR data with those of adducts derived from the reaction between **2** and enol and thioenol ethers.^{4c}

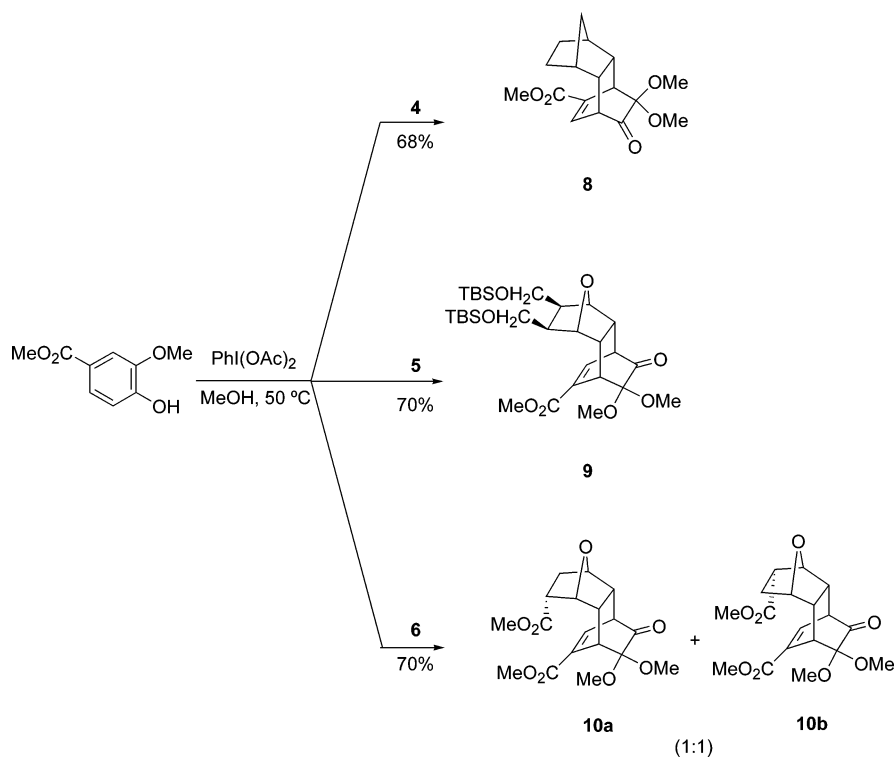
Reactions with the norbornenic derivatives **4–6** were also considered. In our hands, the orthoquinone monoketal **2** reacts with these compounds to give the corresponding tetracyclic cycloadducts **8–10** as a single diastereomer (*endo*) and in acceptable yields (Scheme 3). It should be pointed out that the two possible regioisomers of **10** (**10a** and **10b**) were obtained as an inseparable 1:1 mixture.

Finally, the intramolecular furan–MOB Diels–Alder reaction was considered. Thus, the reaction of methylvanillate with (diacetoxy)iodobenzene in CH₂Cl₂ and in the presence of 2-hydroxymethylfuran gave cycloadduct

SCHEME 2



SCHEME 3



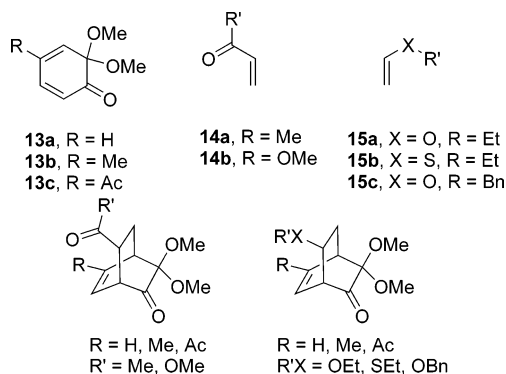
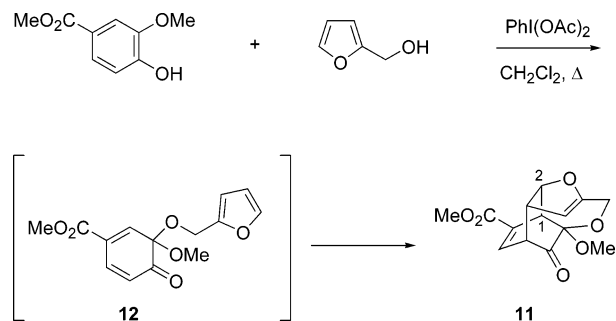


FIGURE 2. Structures of dienes **13a–c**, dienophiles **14** and **15**, and the major adducts resulting from the cycloaddition between them.

SCHEME 4



11 as the only product (47%) (Scheme 4). In this case, the orthoquinone monoketal intermediate **12** undergoes intramolecular Diels–Alder reaction to give the *exo* product by reaction on the unsubstituted double bond of the furan ring.

The structure of **11** was established by ¹H and ¹³C NMR spectral analyses. The signal at 6.30 ppm, corresponding to a single vinylic furan proton, confirms the regioselectivity of the reaction that occurs exclusively at the unsubstituted double bond of the furan ring. On the other hand, the regiochemistry of the cycloaddition was clearly established by ¹H–¹H decoupling experiments. The coupling observed between H-1 (4.19 ppm) and H-2 (4.65 ppm) (Scheme 4) confirms the position of the oxygen atom of the furan ring.

The regioselectivity of the Diels–Alder cycloadditions of dienes **2**, **13b**, and **13c** (Figure 2) with dienophiles **14a** and **14b**, which bear electron-withdrawing substituents, has been analyzed in terms of FMO theory.^{3d} An agreement between ab initio (HF/3-21G*) calculations and experimental results was found only for diene **13b**, which is substituted with a poor electron-donor group (methyl group). When the FMO model was applied to the study of the cycloadditions of dienes **2** and **13a–c**, with dienophiles substituted with electron-donor groups, such as **15c**, the predicted regioselectivity matched the experimental results.^{4a} The main trend predicted for both series of dienophiles, **14** and **15**, was an energetically more favorable interaction between the LUMO of the diene and the HOMO of the dienophile, i.e., the cycloadditions should take place under inverse electron demand.²⁷ However, the energy gaps for both possible HOMO–LUMO interactions between the diene and dienophiles substituted with electron-withdrawing groups were found

to range between 0.3 and 0.7 eV.^{3d} These quite small gaps suggest that both interactions (HOMO–diene–LUMO–dienophile and LUMO–diene–HOMO–dienophile) could be involved and, consequently, prediction of the regioselectivity becomes difficult.

On the other hand, the high *endo* stereoselectivity found in these processes has rarely been studied by a theoretical model.²⁶ Although secondary orbital interactions have been invoked to account for such stereoselectivity,^{3d} additional and probably competitive interactions could be involved in the case of dienophiles with electron-releasing substituents, such as steric interactions between the substituent of the dienophile and the dimethoxy groups in the ethano bridge of the masked *o*-benzoquinones.

Therefore, we hereby describe our ab initio calculations, using a higher basis set (HF/6-31G*) than that used in previous studies,^{3d,4a} of the FMOs of the cycloaddends involved in the cycloadditions under inverse electron demand (IED),^{4c} in order to account for the observed regioselectivity. The FMO energies of the dienes (**2** and **13a**) and dienophiles (**15a,b**) used in our previous report,^{4c} along with those of dienes (**13b,c**) and dienophiles (**14a,b**) recently described in the literature,^{3d} are listed in Table 1. Indeed, a preference for IED is found for the interaction between dienes **2**, **13a**, and **13c** with the dienophiles substituted with electron-withdrawing groups **14a** and **14b** (Table 2, entries 1, 2, 5, 6, 13, and 14). For the reaction of **13b** with dienophiles **14a** and **14b** the normal electron demand (NED) interaction is preferred (Table 2, entries 9 and 10), although the preference is only of 0.1415 and 0.2400 eV, respectively, with respect to the IED interaction.

Table 1 also lists the relative magnitudes of the HOMO and LUMO coefficients of dienes **2** and **13a–c** and dienophiles **14a,b**. The regioselectivity predicted for dienes **2**, **13a**, and **13c** does not agree with the experimental results, except for the interactions between diene **13b** and olefins **14a** and **14b**. These results parallel those reported previously on the basis of 3-21G* calculations.^{3d} The unreliability of the theoretical prediction may be due to the small differences in energy gaps between NED and IED interactions (0.14 to 0.76 eV) (Table 2), leading to an unclear preference between them.

(15) (a) Liu, W. C.; Liao, C. C. *Synlett* **1998**, 912–913. (b) Lee, T. H.; Liao, C. C. *Tetrahedron Lett.* **1996**, *37*, 6869–6872.

(16) Liao, C. C.; Wei, C. P. *Tetrahedron Lett.* **1989**, *30*, 2255–2258.

(17) Liu, W. C.; Liao, C. C. *Chem. Commun.* **1999**, 117–118.

(18) Hsu, D. S.; Hsu, P. Y.; Liao, C. C. *Org. Lett.* **2001**, *3*, 263–265.

(19) Yen, C. F.; Liao, C. C. *Angew. Chem., Int. Ed.* **2002**, *41*, 4090–4093.

(20) Chu, C. S.; Liao, C. C.; Rao, P. D. *Chem. Commun.* **1996**, 1537–1538.

(21) (a) Churcher, I.; Hallett, D.; Magnus P. *Tetrahedron* **1999**, *55*, 1597–1606. (b) Churcher, I.; Hallett, D.; Magnus P. *J. Am. Chem. Soc.* **1998**, *120*, 3518–3519.

(22) Horne, D. A.; Yakushijin, K.; Büchi, G. *Tetrahedron Lett.* **1999**, *40*, 5443–5447.

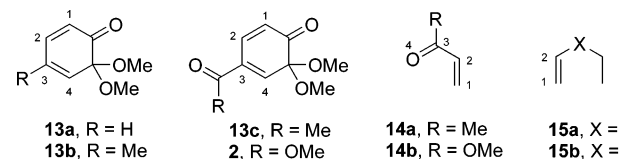
(23) Kürti, L.; Szilágyi, L.; Antus, S. *Eur. J. Org. Chem.* **1999**, 2579–2581.

(24) Njardarson, J. T.; McDonald, I. M.; Spiegel, D. A.; Inoue, M.; Wood, J. L. *Org. Lett.* **2001**, *3*, 2435–2438.

(25) Sutherland, H. S.; Souza, F. E. S.; Rodrigo, R. G. A. *J. Org. Chem.* **2001**, *66*, 3639–3641.

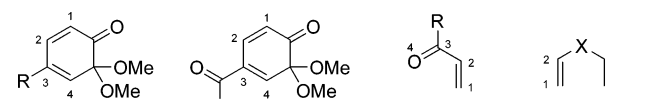
(26) Domingo, L. R.; Aurell, M. J. *J. Org. Chem.* **2002**, *67*, 959–965.

(27) Fleming, I. *Frontier Orbitals and Organic Chemical Reactions*; John Wiley & Sons: Chichester, UK, 1976.

TABLE 1. Ab Initio HF/6-31G* Energies (eV) and Coefficients (C_i) of the Frontier Molecular Orbitals for Dienes **2** and **13a–c** and Dienophiles **14a,b** and **15a,b**^a


compd ^b	HOMO						LUMO					
	<i>E</i>	C_1	C_2	C_3	C_4	ΔC_i^c	<i>E</i>	C_1	C_2	C_3	C_4	ΔC_i^c
2	-9.5241	0.3173	0.2476	-0.2206	-0.2713	0.0460	1.4994	0.1879	-0.2029	-0.1880	0.2882	-0.1003
13a	-9.5186	0.2597	0.1853	-0.2941	-0.2474	0.0123	1.4422	-0.1685	0.2228	0.1230	-0.1923	-0.0238
13b	-9.2084	-0.2890	-0.1943	0.2551	0.3166	-0.0274	1.6463	-0.2009	0.2615	0.1537	-0.2167	-0.0158
13c	-9.7118	0.3145	0.2293	-0.2301	-0.2718	0.0427	1.2463	0.1697	-0.2216	-0.1679	0.2733	-0.1036
14a	-10.3894	0.3391	0.3613	-0.0423	-0.2438	-0.0222	2.6858	0.3105	-0.1961	-0.2947	0.2582	0.1144
14b	-10.6370	0.3432	0.3715	-0.0239	-0.2172	-0.0283	2.8349	0.3295	-0.2249	-0.2840	0.2188	0.1046
15a	-9.0288	0.3810	0.2995			0.0815	5.5267	-0.3053	0.3753			-0.0700
15b	-8.3812	-0.2875	-0.1973			0.0902	4.7620	-0.3247	0.3509			-0.0262

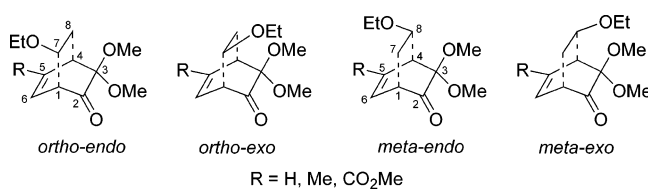
^a These are the values of the p_z coefficients; the relative p_z' contributions and their ΔC_i are analogous. ^b For the most stable planar *s-cis* conformation for olefins **14a** and **14b**. ^c Carbon 1–carbon 2 for the olefins; carbon 1–carbon 4 for the dienes.

TABLE 2. Ab Initio HF/6-31G* Energy Gaps (eV) between the Relevant Frontier Orbitals for Dienes **2** and **13a–c** and Dienophiles **14a,b** and **15a,b**


entry	diene	olefin	NED ^a HOMO–LUMO	IED ^a LUMO–HOMO	diff ^b	interaction ^c
1	2	14a	12.2099	11.8888	0.3211	IED
2	2	14b	12.3590	12.1364	0.2226	IED
3	2	15a	15.0508	10.5282	4.5226	IED
4	2	15b	14.2961	9.8806	4.4155	IED
5	13a	14a	12.2044	11.8316	0.3728	IED
6	13a	14b	12.3535	12.0792	0.2743	IED
7	13a	15a	15.0453	10.4688	4.5765	IED
8	13a	15b	14.2806	9.8234	4.4572	IED
9	13b	14a	11.8942	12.0357	-0.1415	NED
10	13b	14b	12.0433	12.2833	-0.2400	NED
11	13b	15a	14.7351	10.6751	4.0600	IED
12	13b	15b	13.9704	10.0275	3.9489	IED
13	13c	14a	12.3976	11.6357	0.7619	IED
14	13c	14b	12.5467	11.8833	0.6634	IED
15	13c	15a	15.2385	10.2751	4.9634	IED
16	13c	15b	14.4738	9.6275	4.8463	IED

^a HOMO-diene/LUMO-dienophile and LUMO-diene/HOMO-dienophile. ^b (HOMO–LUMO) – (LUMO–HOMO). ^c Electron demand: NED = normal electron demand (HOMO-diene–LUMO-dienophile); IED = inverse electron demand (LUMO-diene–HOMO-dienophile).

In contrast to the above, the difference in energy gaps for the interactions between all of the dienes and the dienophiles substituted with electron-releasing groups, **15a,b**, range from 3.94 to 4.96 eV, clearly indicating a preference for the IED interaction (Table 2). The largest coefficient in the LUMO of the dienes is located at C_4 , while the relative magnitude of the largest coefficient in the HOMO of the dienophiles is located at the double bond terminus C_1 (Table 1). Therefore, the predicted regioselectivity corresponds to the observed *ortho* orientation (Figure 3).

**FIGURE 3.** The four possible transition states for the additions between dienes **2**, **13a**, and **13b** and dienophile **15a**.

Despite the agreement between the predicted and experimental regioselectivity for the strong IED interaction between partners **2**, **13b**, and **13c** and **15a,b**, the FMO model is unable to account for the high *endo* stereoselectivity found for all these cycloadditions, since it is limited to the evaluation of the ground-state interactions. The interactions controlling the *endo* or *exo* selectivity in these processes are the result of a subtle interplay of electronic and steric effects at the transition state (TS). Thus, calculation of the four possible transition states for the reactions between dienes **2**, **13a**, and **13b** and dienophile **15a** were carried out, using the HF/3-21G* level of theory (Figure 3). The energies of the TSS are shown in Table 3.

In contrast to previous calculations of the related cycloaddition of **2** with 2-methylfuran,²⁶ where an intermediate was detected, the potential energy surfaces for each set of four different TSs, corresponding to additions between dienes **2**, **13a**, and **13b** to dienophile **15a**, showed an asynchronous concerted mechanism. In the case of **13a**, the geometries of the two *ortho* TSs (conducting to the observed regioisomers) indicate that the σ bond between carbon C-4 of the diene and carbon C-8 (for numbering, see Figure 3) of the dienophile is more developed than that between carbon C-1 of the diene and C-7 of the olefin (Figure 4), as suggested by the atom distances measured between these reaction centers. In the *meta* TSs, both distances are very similar, suggesting a more synchronous process. The internuclear distances for the addition of **15a** to diene **13b**, in the four TSs, are similar to those shown in Figure 4 for diene **13a** (for example, in the *ortho-endo* TS: $d_{1-7} = 2.552$ Å; $d_{4-8} = 2.024$ Å).

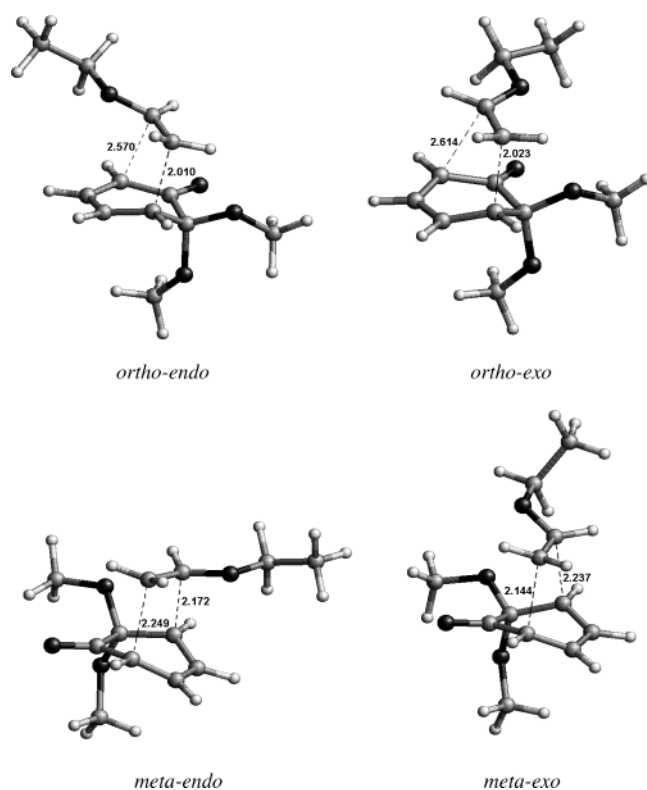


FIGURE 4. Transition states of the four possible approaches for the cycloaddition between diene **13a** and dienophile **15a**.

In the case of the cycloaddition between diene **2** and olefin **15a**, the TSs for the unobserved *meta* adducts were found to be slightly asynchronous as well, with bond distances similar to those found for dienes **13a** and **13b** (for example, in the *meta-endo* TS: $d_{1-7} = 2.321$ Å; $d_{4-8} = 2.111$ Å). However, the asynchrony was much more accentuated for the transition states leading to the *ortho-endo* and *ortho-exo* isomers, as can be seen in the bond distances averaged over the two TSs: $d_{1-7} = 2.9881$ Å and $d_{4-8} = 1.9599$ Å. The latter was quite a bit shorter than those calculated for additions of dienes **13a** and **13b** while the former, d_{1-7} , was much longer (see Figure 4).

This result suggests that in these cases, the cycloadditions proceed through a polar TS, like the one recently calculated for Domingo et al. for the reaction of diene **2** with 2-methylfuran.²⁶ For the reaction between **2** and **15a**, the Mülliken charges determined at the *ortho-endo* TS for carbons C-1 (donor, -0.41) and C-7 (acceptor, 0.34) [C-1 (donor, -0.40) and C-7 (acceptor, 0.33) for the *ortho-exo* TS] would support this hypothesis. However, neither a zwitterionic intermediate nor a second TS were located in the potential energy surface of this reaction. Instead of a second step, the meticulous analysis of the energy surface showed a coherent downward trajectory from the TSs to the adducts. Therefore, we can propose that the cycloadditions conducting to the *ortho* regioisomers proceed via a nonsynchronous concerted pathway, reaching a dipolaroid-like transition state, which leads directly to products, without the presence of a charged intermediate.

It appears then that the concertedness of these processes depends not only on the dienophile, as is the case for 2-methylfuran vs the ethyl vinyl ether (**15a**), but also on the electron demand of the substituents at the diene.

TABLE 3. Ab Initio HF/3-21G Electronic (E_e) and Electronic + Zero-Point Energies (ZPE) (E_0) (au), and Relative Energies (ΔE and ΔE_0)^a (kcal/mol) of the Transition States (TS) for the Cycloaddition of Dienes **2**, **13a**, and **13b** and Dienophile **15a**

diene	TS	E_e	E_0	ΔE_e	ΔE_0
2	<i>ortho-endo</i>	-985.350634	-984.998348	0.000	0.000
2	<i>ortho-exo</i>	-985.346931	-984.995045	2.324	2.073
2	<i>meta-endo</i>	-985.339189	-984.987065	7.182	7.080
2	<i>meta-exo</i>	-985.318261	-984.966944	20.314	19.706
13a	<i>ortho-endo</i>	-759.953175	-759.647365	0.000	0.000
13a	<i>ortho-exo</i>	-759.951876	-759.645854	0.815	0.948
13a	<i>meta-endo</i>	-759.951199	-759.645299	1.240	1.296
13a	<i>meta-exo</i>	-759.932177	-759.626673	13.176	12.984
13b	<i>ortho-endo</i>	-798.773788	-798.438778	0.000	0.000
13b	<i>ortho-exo</i>	-798.772464	-798.437229	0.831	0.972
13b	<i>meta-endo</i>	-798.772639	-798.437324	0.721	0.912
13b	<i>meta-exo</i>	-798.753502	-798.418898	12.730	12.475

^a Relative to the *ortho-endo* TS.

The presence of a stronger electron-withdrawing (methoxycarbonyl) group at C-3 enhances the asynchrony of the reaction, particularly for the *ortho* approaches. This may be interpreted in terms of the synergistic effects of the methoxycarbonyl at C-5 and the carbonyl group at C-2, which reduce the electron density at C-4 (see Table 2), increasing at the same time the positive charge at this position. Thus, a stronger interaction would be expected between C-4 in the MOB and C-8 in **15a** (Figure 3), which is the more electron-rich position in the double bond of the dienophile.

From the electronic energies obtained for the additions of the three dienes, it turned out that the *ortho-endo* TS was more stable than the *ortho-exo* TS (Table 3). The electronic energies including the zero-point energy correction (E_0) are also shown in Table 3, and their values suggest a preference for the *ortho-endo* TS of ca. 0.96 kcal/mol for **13a** and **13b**, while the difference is larger (2.07 kcal/mol) for diene **2** (Table 3). Moreover, the relative magnitude of the TS energies for the corresponding *meta* regioisomers leads to a similar prediction: the *endo* TS should be more stable than the *exo* TS.

Even though the electronic energy differences (ΔE) between the *ortho-endo/ortho-exo* TSs for dienes **13a** and **13b** are relatively small, a preferential trend for the *endo* TS is found. The magnitude of the ΔE for diene **2** is, however, larger, indicating a clear preference for the *ortho-endo* approach. The ΔE_0 is slightly more differentiated with respect to the stability of the TSs for the *ortho/meta* regioisomers for diene **13a**. For the *endo* approaches, the *ortho* isomer was ca. 1.30 kcal/mol more stable than the *meta* TS (Table 3). This difference is largely enhanced (ca. 7.08 kcal/mol) for diene **2**. This was not the case for diene **13b**, which is slightly smaller. However, in all cases a much larger difference was calculated for the *meta-exo* approaches, with respect to the energetically more stable *ortho-endo* TS. Therefore, it is clear that these TS calculations agree with the FMO prediction for an *ortho* preference, as experimentally observed.

Secondary orbital interactions have been invoked to explain the *endo* preference, even for dienophiles bearing

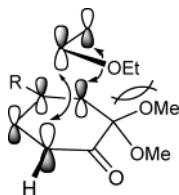


FIGURE 5. Interaction sites in the *ortho-exo* Diels–Alder transition state for the addition between dienes **2**, **13a**, and **13b**, with dienophile **15a**.

electron-donating groups.²⁸ In our case, however, the geometries of the *endo* TSs do not show any particularly short distance between the diene and the ether group of the dienophile that could reveal a possible secondary interaction.

It seems that, for our additions, steric interactions²⁹ developed at the *exo* TS between the ethoxy (or thioethoxy) group of the vinyl ether (or vinyl thioether) of the dienophile and those of the ketal substituent on the ethano bridge of the diene can destabilize such an approach (Figures 4 and 5), favoring the *endo* TS. This factor could also explain the high energies calculated for the *meta-exo* TSs, where the alkoxy groups of diene and dienophile are in close proximity, thus enhancing the van der Waals interactions.

Conclusions

The Diels–Alder reactions of the masked *o*-benzoquinone **2** with new electron-rich dienophiles, including bicyclic systems, have been studied. In addition, we describe for the first time the intramolecular Diels–Alder reaction of furan and a MOB. It should be pointed out that this process occurs with total regio- and stereoselectivity.

The FMO model allows us to predict the correct regioselectivity for the Diels–Alder cycloadditions of dienes, **2** and **13a–c**, with the dienophiles substituted by strong electron-releasing groups, **15a,b**, under inverse electron-demand conditions. However, this theoretical approach fails to rationalize the orientation observed with dienophiles substituted with electron-withdrawing groups, such as **14a** and **14b**. Ab initio calculations of the four possible transition states for the cycloaddition of diene **13a** with dienophile **15a** provide a rationalization of the regioselectivity and the high *endo* stereoselectivity experimentally observed. In addition, these calculations suggest that an asynchronous concerted transition state is involved in this type of process.

Experimental Section

Reagents obtained from commercial sources were used as received, and solvents were dried prior to use. Silica gel 60 F₂₅₄ was used for TLC, and the spots were detected with UV or KMnO₄ solution. Flash column chromatography was carried out on silica gel 60. IR spectra have been recorded as CHCl₃

solutions. ¹H and ¹³C NMR spectra were recorded at 300 and 50 MHz, respectively, in CDCl₃ solution with TMS as internal reference.

The ab initio calculations were carried out with the Gaussian 94 program package³⁰ running on personal computers under the Linux operating system. Preliminary geometry optimizations of the starting materials and products were carried out first with the AM1 semiempirical method, and these geometries were employed as starting points for optimization with the HF/3-21G and HF/6-31G* models. FMO energies and coefficients were determined at the HF/6-31G* level of theory. Characterization of the potential energy surface of this process was carried out with the HF/3-21G model. Optimization of reactants, products, and transition states was followed by frequency analysis to ensure the correct nature of the stationary points. For the transition states, the normal modes corresponding to the imaginary frequencies were analyzed visually to confirm that they led to the desired products. For the particular case of both *ortho* approaches in the reaction between **2** and **15a**, IRC calculations were carried out, starting from the corresponding transition states, as well as an extensive potential surface scan (HF/3-21G); no additional stationary points were located.

Synthesis of 2,3-*exo*-Bis(*tert*-butyldimethylsilyloxymethyl)-7-oxabicyclo[2.2.1]hept-5-ene, **5.** To a solution of 7-oxabicyclo[2.2.1]hept-5-ene-*cis-exo*-2,3-dimethanol³¹ (490 mg, 3.14 mmol) in 31 mL of CH₂Cl₂ were added 1.09 mL (7.85 mmol) of Et₃N and 1.8 mL (7.85 mmol) of *tert*-butyldimethylsilyl trifluoromethanesulfonate. After the mixture was stirred for 1 h, the reaction was quenched with K₂CO₃, 5% aqueous NaHCO₃, and water and extracted with CH₂Cl₂. The combined organic layers were dried over MgSO₄ and concentrated to give a crude residue, which was purified by column chromatography (hexane:EtOAc 10:1) to afford 936 mg of **5** as a pale yellow oil (78%). IR (CHCl₃) ν 1637, 1257, 1047 cm⁻¹. ¹H NMR (CDCl₃, 300 MHz) δ 0.06 (s, 6 H), 0.07 (s, 6 H), 0.91 (s, 18 H), 1.78 (t, 2 H, *J* = 5.4 Hz), 3.54 (t, 2 H, *J* = 9.3 Hz), 3.77 (dd, 2 H, *J* = 5.4, 9.3 Hz), 4.82 (s, 2 H), 6.35 (s, 2 H). ¹³C NMR (CDCl₃, 50 MHz) δ -5.3, -5.3, 25.7, 25.9, 42.5, 62.4, 80.4, 135.5. Anal. Calcd for C₂₀H₄₀O₃Si₂: C, 62.50; H, 10.42. Found: C, 62.63; H, 10.34.

Synthesis of 7-Oxabicyclo[2.2.1]hept-5-ene-2-*endo*-carboxylic Acid Methyl Ester, **6.** To a solution of 7-oxabicyclo[2.2.1]hept-5-ene-2-*endo*-carboxylic acid³² (1.91 g, 13.6 mmol) and MeOH (0.6 mL, 15 mmol) in 41 mL of CH₂Cl₂ cooled to 0 °C was added a solution of 1,3-dicyclohexylcarbodiimide (2.8 g, 13.6 mmol) and (dimethylamino)pyridine (17 mg, 0.14 mmol) in CH₂Cl₂ (41 mL) dropwise. The reaction mixture was stirred for 24 h and then filtered, washed with Et₂O, and concentrated. The residue was purified by chromatography (hexane:Et₂O 5:1) to afford 1.26 g of **6** as a pale yellow oil (60%). IR (CHCl₃) ν 2849, 1736, 1630, 1132 cm⁻¹. ¹H NMR (CDCl₃, 300 MHz) δ 1.52 (dd, 1 H, *J* = 3.9, 11.2 Hz), 2.04 (ddd, 1 H, *J* = 4.9, 9.3, 11.2 Hz), 3.06 (dt, 1 H, *J* = 4.9, 9.1 Hz), 3.58 (s, 3 H), 4.96 (dd, 1 H, *J* = 1.2, 4.6 Hz), 5.10 (dd, 1 H, *J* = 1.5, 4.9 Hz), 6.16 (dd, 1 H, *J* = 1.5, 5.9 Hz), 6.38 (dd, 1 H, *J* = 1.5, 5.9 Hz). ¹³C NMR (CDCl₃, 50 MHz) δ 28.3, 42.4, 51.5, 78.5, 78.7, 132.3, 136.8, 172.3. Anal. Calcd for C₈H₁₀O₃: C, 62.34; H, 6.49. Found: C, 62.43; H, 6.35.

Synthesis of Bicyclo[2.2.2]octenones 7–10: General Procedure. A solution of methylvanillate (0.4 mmol) and the

(30) Frisch, M. J.; Trucks, G. W.; Schlegel, H. B.; Gill, P. M. W.; Johnson, B. G.; Robb, M. A.; Cheeseman, J. R.; Keith, T.; Petersson, G. A.; Montgomery, J. A.; Raghavachari, K.; Al-Laham, M. A.; Zakrzewski, V. G.; Ortiz, J. V.; Foresman, J. B.; Cioslowski, J.; Stefanov, B. B.; Nanayakkara, A.; Challacombe, M.; Peng, C. Y.; Ayala, P. Y.; Chen, W.; Wong, M. W.; Andres, J. L.; Replogle, E. S.; Gomperts, R.; Martin, R. L.; Fox, D. J.; Binkley, J. S.; Defrees, D. J.; Baker, J.; Stewart, J. P.; Head-Gordon, M.; Gonzalez, C.; Pople, J. A. *Gaussian 94*; Gaussian, Inc.: Pittsburgh, PA, 1995.

(31) Das, J.; Vu, T.; Harris, D. N.; Ogletree, M. L. *J. Med. Chem.* **1988**, *31*, 930–935.

(32) Moore, J. A.; Partain, E. M., III *J. Org. Chem.* **1983**, *48*, 1105–1106.

(28) (a) Apeloig, Y.; Matzner, E. *J. Am. Chem. Soc.* **1995**, *117*, 5375–5376. (b) Arrieta, A.; Cossio, F. P.; Lecea, B. *J. Org. Chem.* **2001**, *66*, 6178–6180. (c) Caramella, P.; Quadrelli, P.; Toma, L. *J. Am. Chem. Soc.* **2002**, *124*, 1130–1131.

(29) (a) Cantello, B. C. C.; Mellor, J. M.; Webb, C. F. *J. Chem. Soc., Perkin Trans. 2* **1974**, 22–25. (b) Fringuelli, F.; Guo, M.; Minuti, L.; Pizzo, F.; Taticchi, A.; Wenkert, E. *J. Org. Chem.* **1989**, *54*, 710–712.

corresponding dienophile (10 mmol) in 1.2 mL of MeOH was heated to 50 °C. Then, 1.2 mmol of (diacetoxy)iodobenzene in 3.6 mL of MeOH was added via a syringe pump over 1.5 h. After the mixture was stirred for 10 min, the solvent was removed under reduced pressure. The residue was purified by chromatography (hexane:EtOAc 10:1).

(1R*,2S*,6R*,7S*)-11,11-Dimethoxy-4,10-dioxo-3,5-dioxatricyclo[5.2.2.0^{2,6}]undec-8-ene-8-carboxylic Acid Methyl Ester, 7. Pale yellow oil, 27%. IR (CHCl₃) ν 2852, 1751, 1718, 1630 cm⁻¹. ¹H NMR (CDCl₃, 300 MHz) δ 3.36 (s, 3 H), 3.37 (s, 3 H), 3.84 (s, 3 H), 3.92–3.95 (m, 1 H), 4.39 (m, 1 H), 5.08 (dd, 1 H, J = 2.7, 7.8 Hz), 5.33 (dd, 1 H, J = 3.7, 7.8 Hz), 7.17 (d, 1 H, J = 4.4 Hz). ¹³C NMR (CDCl₃, 50 MHz) δ 31.9, 42.0, 50.3, 52.6, 53.4, 73.6, 74.1, 92.5, 133.9, 135.0, 153.5, 163.0, 194.3. Anal. Calcd for C₁₃H₁₄O₈: C, 52.35; H, 4.70. Found: C, 52.27; H, 4.61.

(1R*,2R*,3R*,6S*,7S*,8R*)-13-Methane-12,12-dimethoxy-11-oxotetracyclo[6.2.2.1^{3,6}.0^{2,7}]tridec-9-ene-9-carboxylic Acid Methyl Ester, 8. Pale yellow oil, 68%. IR (CHCl₃) ν 2837, 1740, 1713, 1296 cm⁻¹. ¹H NMR (CDCl₃, 300 MHz) δ 0.76 (d, 1 H, J = 10.1 Hz), 1.11–1.27 (m, 2 H), 1.45 (dd, 2 H, J = 4.4, 12.7 Hz), 1.72 (d, 1 H, J = 10.1 Hz), 2.08 (dd, 1 H, J = 1.5, 8.8 Hz), 2.15 (br s, 1 H), 2.20 (br s, 1 H), 2.23 (dd, 1 H, J = 2.9, 8.3 Hz), 3.24 (s, 3 H), 3.38 (s, 3 H), 3.36–3.39 (m, 1 H), 3.81 (s, 3 H), 3.81–3.82 (m, 1 H), 7.05 (dd, 1 H, J = 1.5, 7.5 Hz). ¹³C NMR (CDCl₃, 50 MHz) δ 30.4, 31.6, 35.6, 40.4, 41.1, 42.1, 42.9, 45.3, 49.9, 50.3, 52.0, 54.1, 94.2, 136.3, 137.4, 164.6, 200.5. Anal. Calcd for C₁₇H₂₂O₅: C, 66.67; H, 7.19. Found: C, 66.78; H, 7.31.

(1S*,2S*,3R*,4S*,5R*,6R*,7R*,8S*)-4,5-Bis(tert-butyl-dimethylsilyloxymethyl)-12,12-dimethoxy-11-oxo-13-oxatetracyclo[6.2.2.1^{3,6}.0^{2,7}]tridec-9-ene-9-carboxylic Acid Methyl Ester, 9. Pale yellow oil, 70%. IR (CHCl₃) ν 2858, 1736, 1711, 1259 cm⁻¹. ¹H NMR (CDCl₃, 300 MHz) δ 0.01 (s, 6 H), 0.02 (s, 6 H), 0.87 (s, 9 H), 0.88 (s, 9 H), 1.94–2.08 (m, 2 H), 2.38 (dd, 1 H, J = 1.9, 8.3 Hz), 2.55 (dd, 1 H, J = 2.9, 8.3 Hz), 3.26 (s, 3 H), 3.43–3.34 (m, 1 H), 3.38 (s, 3 H), 3.47 (dd, 1 H, J = 2.9, 6.8 Hz), 3.45–3.53 (m, 1 H), 3.56–3.58 (m, 2 H), 3.79 (s, 3 H), 3.93 (t, 1 H, J = 2.4 Hz), 4.16 (s, 1 H), 4.23 (s, 1 H), 7.04 (dd, 1 H, J = 1.5, 6.8 Hz). ¹³C NMR (CDCl₃, 50 MHz) δ -5.4, -5.4, 18.1, 18.2, 25.8, 25.9, 41.9, 42.0, 44.8, 49.5, 50.1, 50.2, 52.0, 52.8, 60.4, 60.6, 60.9, 82.1, 82.9, 93.8, 134.0, 135.1, 164.8, 199.8. Anal. Calcd for C₃₀H₅₂O₈Si₂: C, 60.40; H, 8.72. Found: C, 60.54; H, 8.61.

(1S*,2S*,3S*,5R*,6R*,7R*,8S*)-12,12-Dimethoxy-5-endo-(methoxycarbonyl)-11-oxo-13-oxatetracyclo[6.2.2.1^{3,6}.0^{2,7}]-

tridec-9-ene-9-carboxylic Acid Methyl Ester, 10a, and (1S*,2S*,3R*,4S*,6S*,7R*,8S*)-12,12-Dimethoxy-4-endo-(methoxycarbonyl)-11-oxo-13-oxatetracyclo[6.2.2.1^{3,6}.0^{2,7}]-tridec-9-ene-9-carboxylic Acid Methyl Ester, 10b. Pale yellow oil, 70%. IR (CHCl₃) ν 2839, 1736, 1161, 1146 cm⁻¹. ¹H NMR (CDCl₃, 300 MHz) δ 2.00–1.82 (m, 4 H), 2.44–2.39 (m, 2 H), 2.62 (dd, 2 H, J = 2.9, 7.8 Hz), 3.00–2.91 (m, 2 H), 3.25 (s, 6 H), 3.34 (s, 3 H), 3.37 (s, 3 H), 3.42 (dd, 1 H, J = 2.4, 6.3 Hz), 3.46 (dd, 1 H, J = 2.4, 6.3 Hz), 3.71 (s, 3 H), 3.74 (s, 3 H), 3.79 (s, 3 H), 3.80 (s, 3 H), 3.87 (t, 1 H, J = 2.4 Hz), 3.92 (t, 1 H, J = 2.4 Hz), 4.39 (d, 2 H, J = 4.4 Hz), 4.51 (d, 2 H, J = 5.9 Hz), 7.03 (dt, 2 H, J = 2.4, 6.3 Hz). ¹³C NMR (CDCl₃, 50 MHz) δ 33.4, 34.0, 38.4, 41.5, 41.9, 42.1, 42.3, 45.3, 47.9, 48.2, 50.0, 50.1, 50.3, 52.0, 52.1, 52.2, 52.4, 52.8, 80.5, 81.1, 81.2, 81.6, 93.7, 93.7, 134.4, 135.0, 135.1, 164.8, 171.9, 172.0, 199.3. Anal. Calcd for C₁₈H₂₂O₈: C, 59.02; H, 6.01. Found: C, 58.93; H, 6.12.

Synthesis of (1R*,2S*,7S*,9S*,12S*)-7-Methoxy-8-oxo-3,6-dioxatetracyclo[5.4.2^{1,9}.1^{4,12}.0^{1,7}]trideca-4,10-diene-11-carboxylic Acid Methyl Ester, 11. A solution of (diacetoxy)iodobenzene (198 mg, 0.61 mmol) and 2-hydroxymethylfuran (0.65 mL, 7.5 mmol) in CH₂Cl₂ (0.8 mL) was heated to reflux. Then, methylvanillate (75 mg, 0.41 mmol) in 0.6 mL of CH₂-Cl₂ was added via a syringe pump over 3 h. After being stirred 12 h at reflux, the reaction mixture was quenched with saturated aqueous NaHCO₃ and saturated aqueous NaCl and extracted with CH₂Cl₂. The combined organic layers were dried over MgSO₄ and concentrated to give a crude residue, which was purified by column chromatography (hexane:EtOAc 5:1) to afford 53 mg of **11** as a pale yellow oil (47%). IR (CHCl₃) ν 2856, 1751, 1718, 1138 cm⁻¹. ¹H NMR (CDCl₃, 300 MHz) δ 3.54 (s, 3 H), 3.71 (dd, 1 H, J = 3.3, 7.0 Hz), 3.77–3.81 (m, 1 H), 3.83 (s, 3 H), 3.95 (d, 1 H, J = 7.4 Hz), 4.18 (d, 1 H, J = 7.5 Hz), 4.19 (d, 1 H, J = 1.9 Hz), 4.65 (t, 1 H, J = 2.2 Hz), 6.30 (dd, 1 H, J = 2.2, 2.9 Hz), 7.02 (dd, 1 H, J = 2.2, 7.0 Hz). ¹³C NMR (CDCl₃, 50 MHz) δ 45.4, 50.9, 51.5, 52.8, 72.6, 77.6, 89.4, 97.5, 99.8, 132.1, 137.8, 149.1, 164.6, 198.9. Anal. Calcd for C₁₄H₁₄O₆: C, 60.43; H, 5.03. Found: C, 60.52; H, 4.91.

Acknowledgment. The Ministerio de Ciencia y Tecnología of Spain (Project BQU2000-0653) is gratefully thanked for financial support. J.T. and H.A.J.-V. are fellows of the EDD/IPN and COFAA/IPN programs.

JO030307R